Appendix A

Testing of the template model using Vision Egg software

A.1 Vision Egg

Recent advances in computer technology make it possible to produce visual stimuli not previously possible. Arbitrary scenes, from traditional sinusoidal gratings to naturalistic 3D scenes can now be specified on a frame-by-frame basis in realtime with modern graphics hardware. Andrew Straw developed a programming library called the Vision Egg that makes it easy to take advantage of these innovations. The Vision Egg is free, open-source software making use of OpenGL and written in the high-level language Python with extensions in C code. Careful attention has been paid to the issues of calibration and hardware interfacing, making the Vision Egg suitable for psychophysical, electrophysiological, and behavioral experiments [Straw, 2004].

A.2 Measuring angular velocity

Recall that in Chapter 2, we performed an experiment using a rotating drum to measure angular velocity using the template model. This had difficulty in recording the speed control uniformly. Therefore the experiment is repeated using the Vision Egg software to demonstrate improved results. The results are repeated from Chapter 2 to compare it with the Vision Egg results.

A.2.1 Using a rotating drum

We have set up an experiment to test the effectiveness of different de-noising algorithms. In this experiment, the camera was placed in the center of a white hollow cylinder with a vertical black paper bar inside. The cylinder is motor controlled and the angular speed of the cylinder can be adjusted by changing the voltage supply to the motor. Our program then tried to measure the angular speed of the cylinder by detecting the motion of the dark paper. The black paper is used to measure the angular velocity of the luminance templates. The experiment is repeated with red and blue paper stripes to measure the angular velocities of the red and blue chrominance templates respectively.

Experimental results show that a moving object (or edge) consistently causes the same motion sensitive template to occur at subsequent time steps, and at positions corresponding to the displacement of the edge relative to the detector [Yakovleff et al., 1994]. The angular velocity may be estimated by evaluating the ratio of the displacement of a motion sensitive template, to the time between the template's occurrences (i.e., in Figure 2.11, the angular velocity is angular displacement/ΔT).

The rotating speed was increased from 10 rpm to 45 rpm in steps of 5 rpm. The horizontal axis represents real speed in rpm (varying from 10 rpm to 45 rpm), which was measured by using a tachometer. The vertical axis represents speed in rpm (varying from 10rpm to 45 rpm) measured using our program.

A.2.2 Using Vision Egg software

In this method, we used two computers, one which is the video capture computer that hosts our insect vision software (template model) and the other computer which we call the Vision Egg stimuli computer which generates the rotating stimuli which is used instead of the drum and which runs images on Vision Egg. It uses the python programming language to create different kinds of moving visual stimuli that can be very useful for the vision community. Many of the physiological experimental results obtained in this Thesis used this software for generating stimuli for the electro-physiological experiments. The Vision Egg software simulates a rotating drum and the images are rotated across the LCD screen. The CMOS camera mounted on a retort stand captures the moving images and sends the captured frames to the video capture computer for the insect vision software to perform analysis and motion detection. The video capture computer also has an EPIX SV4 image capture card installed in it and it acts as an interface for the CMOS camera to send captured images to the computer. The CMOS camera is placed at about 17 cm away from the LCD screen so that it could capture a larger area of the rotating drum without capturing anything outside of it. To reduce the effect of ceiling lights on our experiments, the CMOS camera and LCD screen are covered using a book or box [Budimir et al., 2004; Guzinski et al., 2006].

The experiments performed with the rotating drum are repeated by placing the camera in front of a computer with a Vision Egg software running on it (See Chapter 2).

There are two algorithms for estimating velocity in real-time that have been developed and tested. The first algorithm is forward tracking [Yakovleff et al., 1995], and the second algorithm is stair-step tracking [Nguyen et al., 1993]. In this experiment, the forward tracking algorithm for velocity measurement is used. In the forward tracking algorithm, certain motion templates are tracked within a fixed time "window" of previous (small) displacements, and of the time steps at which they occurred, the velocity is provided by the ratio of the sum of the displacements, to the size of the window. Using this method, the velocity of a slow moving object is determined and updated at each sampling instant. In theory, this makes it more useful in counting templates for objects moving at low velocities [Nguyen et al., 1996].

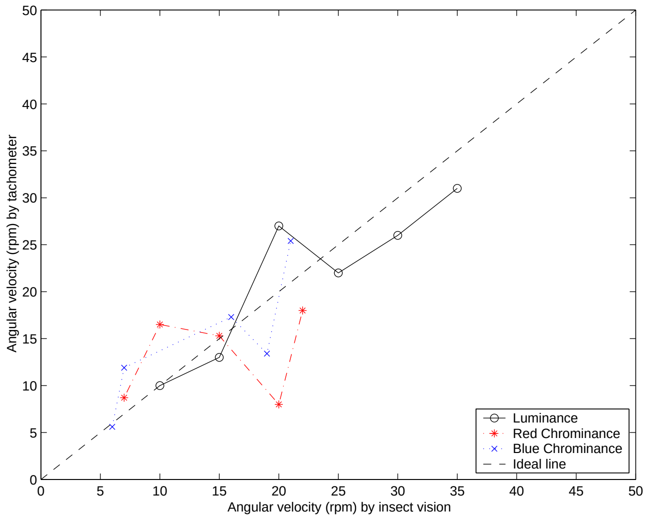

Fig. A.1. Comparison of angular velocity curves with no pre-filtering using the rotating drum. Benchmark angular velocity measured by a tachometer versus angular velocity determined by insect vision system. Case 1: Without using any noise removal algorithms. Frame rate was 60 ms.

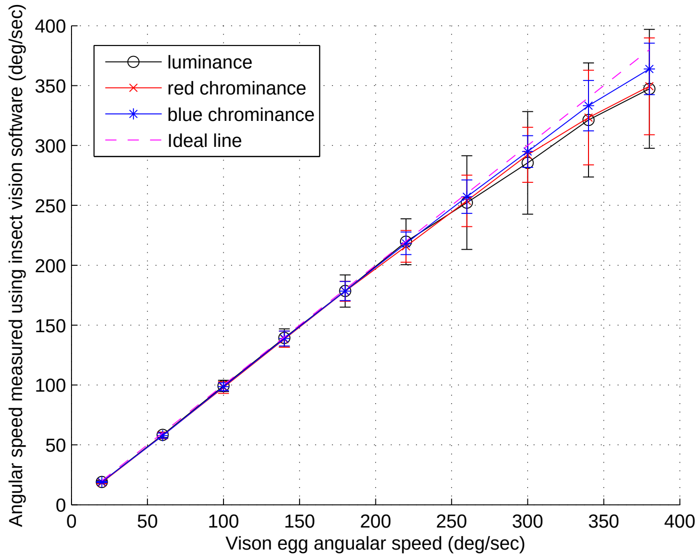

Fig. A.2. Comparison of angular velocity curves with no pre-filtering using the Vision Egg software. Benchmark angular velocity measured by the Vision Egg algorithm versus angular velocity determined by insect vision system. Case 1: Without using any noise removal algorithms.

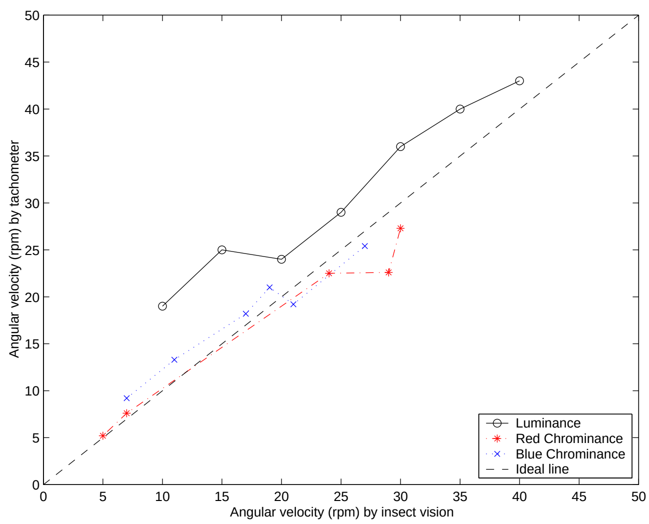

Fig. A.3. Comparison of angular velocity curves with spatial averaging using the rotating drum. Benchmark angular velocity measured by a tachometer versus angular velocity determined by insect vision system. Case 2: Using the spatial averaging algorithm. Frame rate was 60 ms.

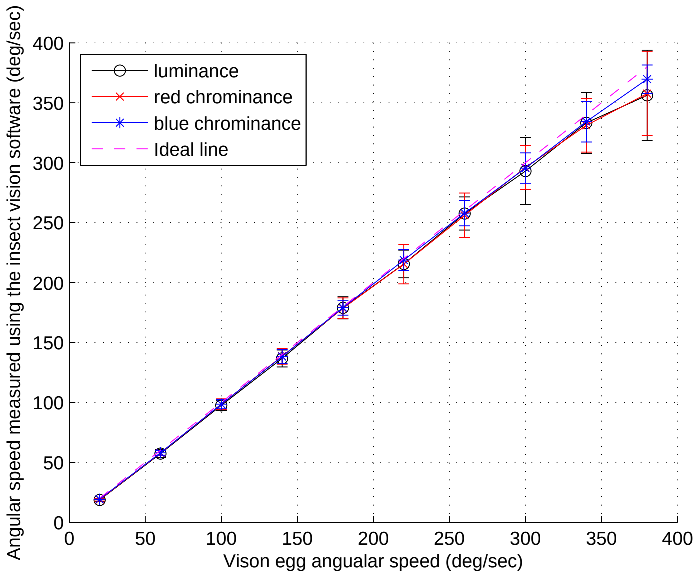

Fig. A.4. Comparison of angular velocity curves with spatial averaging using the Vision Egg software. Benchmark angular velocity measured by the Vision Egg software versus angular velocity determined by insect vision system. Case 2: Using the spatial averaging algorithm. Frame rate was 60 ms.

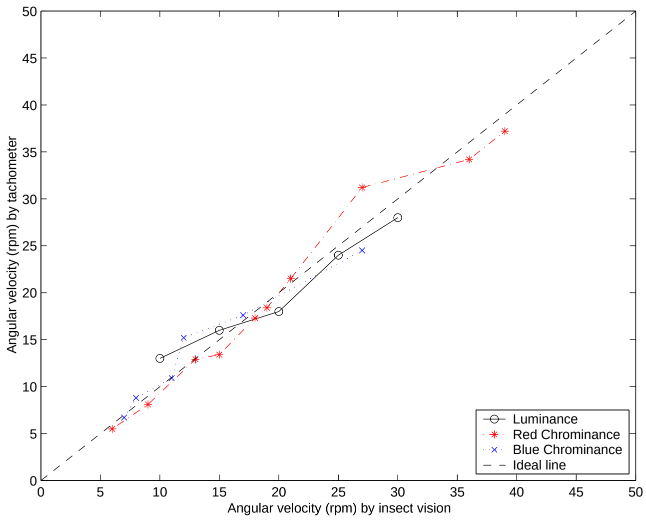

Fig. A.5. Comparison of angular velocity curves with MNC filtering using the rotating drum. Benchmark angular velocity measured by a tachometer versus angular velocity determined by insect vision system. Case 3: Using the MNC method. Frame rate was 60 ms.

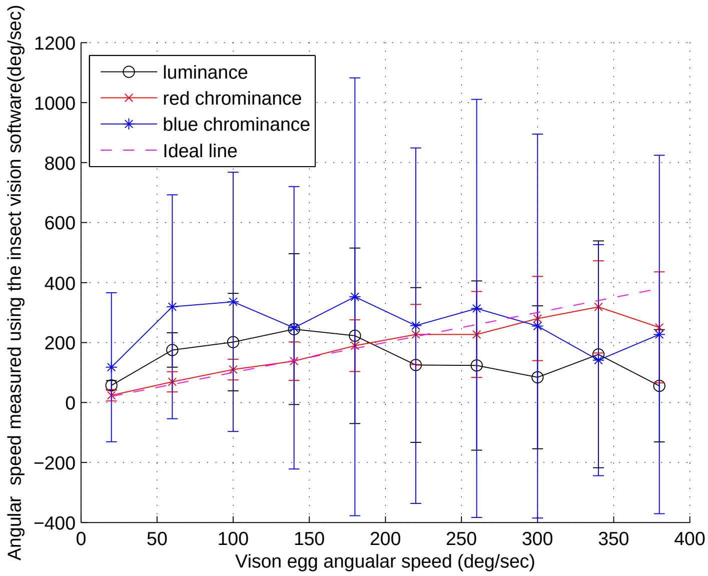

Fig. A.6. Comparison of angular velocity curves with MNC filtering using the Vision Egg software. Benchmark angular velocity measured by the Vision Egg software versus angular velocity determined by insect vision system. Case 3: Using the MNC method.

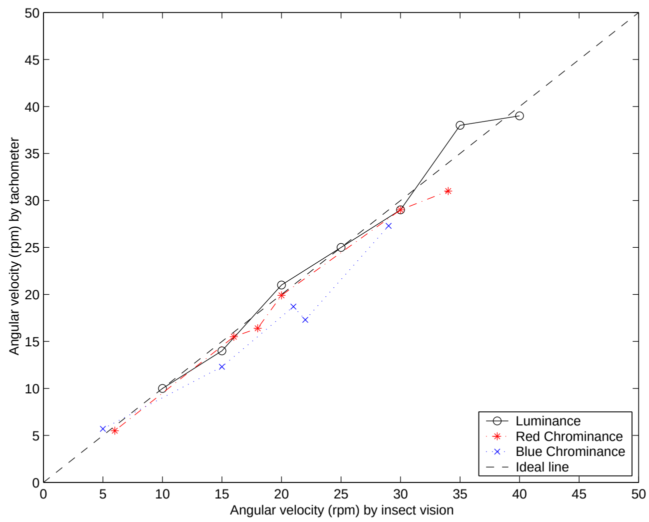

Fig. A.7. Comparison of angular velocity curves with template pair filtering using the rotating drum. Benchmark angular velocity measured by a tachometer versus angular velocity determined by insect vision system. Case 4: Using the template pair method. Frame rate was 60 ms.

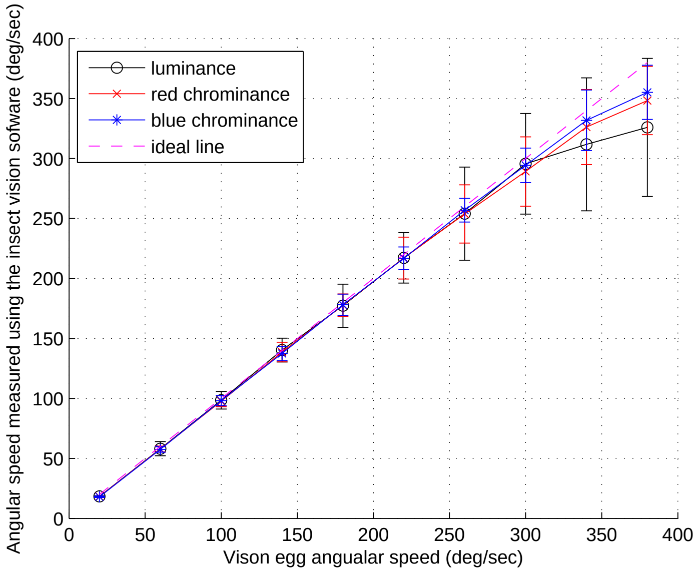

Fig. A.8. Comparison of angular velocity curves with template pair filtering using the Vision Egg software. Benchmark angular velocity measured by the Vision Egg algorithm versus angular velocity determined by insect vision system. Case 4: Using the template pair method. Frame rate was 60 ms.

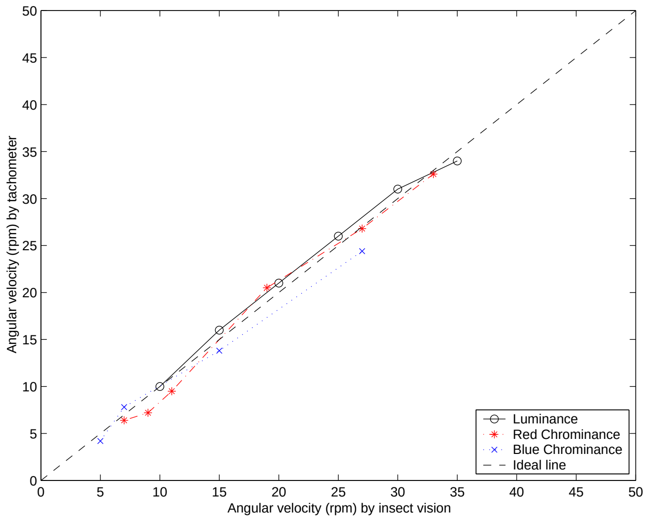

Fig. A.9. Comparison of angular velocity curves with averaging and template pair method. Benchmark angular velocity measured by a tachometer versus angular velocity determined by insect vision system. Case 6: Using the averaging and template pair technique. Frame rate was 60 ms.

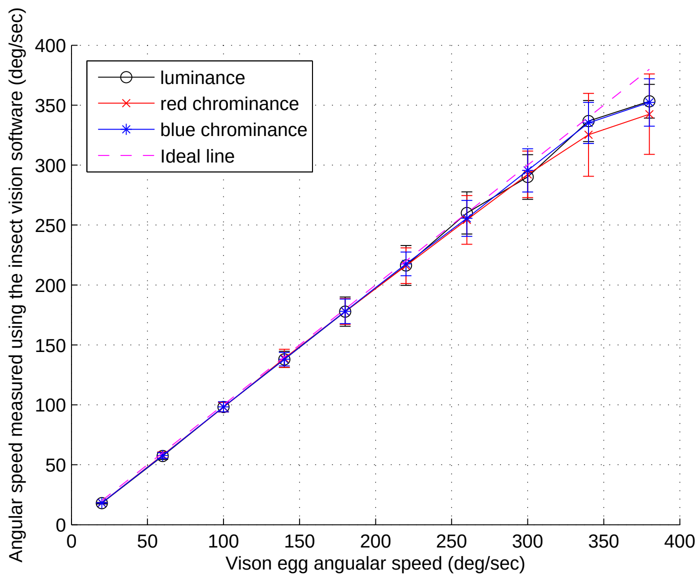

Fig. A.10. Comparison of angular velocity curves with the averaging and template pair method using the Vision Egg software. Benchmark angular velocity measured by the Vision Egg software versus angular velocity determined by insect vision system. Case 5: Using the averaging and template pair technique.

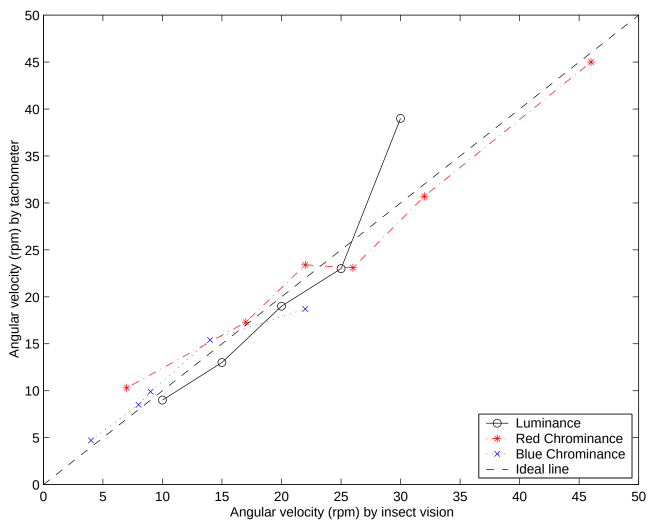

Fig. A.11. Comparison of angular velocity curves with MNC and template pair technique. Benchmark angular velocity measured by a tachometer versus angular velocity determined by insect vision system. Case 8: Using the MNC and template pair technique. Frame rate was 60 ms.

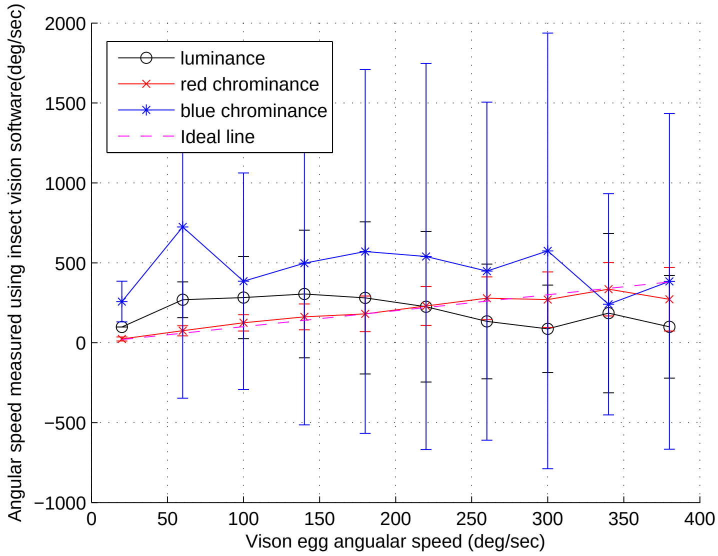

Fig. A.12. Comparison of angular velocity curves with MNC and template pair technique. Benchmark angular velocity measured by a tachometer versus angular velocity determined by insect vision system. Case 8: Using the MNC and template pair technique. Frame rate was 60 ms.

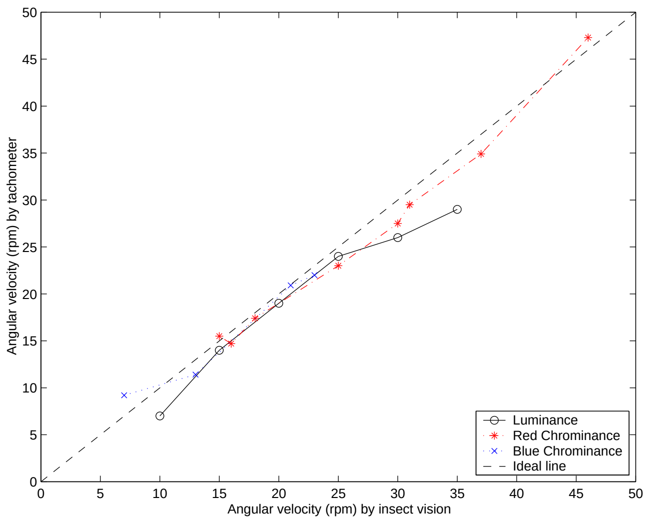

Fig. A.13. Comparison of angular velocity curves with windowing method. Benchmark angular velocity measured by a tachometer versus angular velocity determined by insect vision system. Case 5: Using the windowing method. Frame rate was 60 ms. This experiment was done using the Vision Egg stimuli as we found that the template pair algorithm gives better results than the windowing method.

A.2.3 Analysis of Results

Results from the experiments are shown in Figures A.1 to A.13.

Figure A.1 shows that without applying any filtering process the response scatters randomly around the ideal response. Figure A.2 gives a much better result compared that obtained using a drum and this could be due to the use of the rotating cylinder which might not have rotated at consistent speeds and thus have affected the results. Results from Figure A.3 and Figure A.4 show that the averaging process helps in smoothing the response in both the cases. Figure 2.3 and Figure A.6 indicates that the measured speeds are shifting up from the ideal response. This can be explained by the calculation errors (division) of the digital computer. In this stage noise is sometimes amplified to a point where it dominates the signals induced by the motion of objects. In this filter we again averaged the luminance (chrominance) values over three receptors adjacent in the horizontal plane. Dividing a value by the average gives a result centered on 1. In the Template model implementation this result is not very useful as the change in intensity detected by the receptor over one frame must be larger then the threshold before that change is recognized. The minimum value of the threshold is 1 so no change in intensity and templates would ever be detected. To overcome this, the result of MNC filtering was scaled up by multiplying it by a constant value of a 100.

Figure A.13 indicates that applying the windowing operation to the templates helps in eliminating the constantly varying nature of the response. This is due to the local nature of the windowing algorithm. The template-pairs algorithm produces similar performance to the windowing algorithm, but the result is much more consistent. Since the windowing algorithm seems to leave noise in the result wherever the noisy templates are surrounded by other templates, this method is not included in the Vision Egg experiments.

Figure A.9, Figure A.10, Figure A.11 and Figure A.12 are combinations of pre-template filtering and post-template filtering. These figures indicate significant improvement in performance compared to using each individual technique or not using any technique at all. This result demonstrates that the pre-filtering techniques and the post filtering techniques do actually combine well in eliminating noise. From these experiments it can be seen that combining averaging, during pre-template filtering, and conjugate-pair techniques, during post-template filtering give the best overall response. However many more experiments with different conditions need to be carried out before such general conclusion can be reached.

In all the cases it is seen that the results obtained with the Vision Egg software gave better results than that using the drum and the reason for the inconsistency and variations of results could be the inconsistent angular speed of the stimuli. The angular speed of the stimuli is controlled by the voltage supply to the motor, thus the speed of the stimuli might not be as consistent or accurate.

The graph shows that the speed estimation algorithm works perfectly up to around 250°/s with the Vision Egg software. After that the detected speed drops slightly below the actual speed but is still quite accurate up to around 350°/s. It is especially good when looking at blue chrominance. It could be argued that in this case the filters were not needed at all. However it is still important to see if they improve the accuracy at higher speeds and check that they do not deteriorate the accuracy at lower ones.

The results show that the speed estimation algorithm is most accurate when the spatial averaging filter is used. This is not a surprising result as that filter is commonly used in other applications. Instead of implementing the filter in software, and thus using up CPU time, it is also possible to implement it in hardware by changing the focus of the camera lens so that the picture recorded is slightly blurred.

The MNC filter is not suitable for this application, as it introduces a lot of noise and destroys the precision of the system. This is caused by the fact that to use this filter in this application the values have to be multiplied after filtering by a 100 and the threshold set to 1. This first operation amplifies any remaining noise and the second one lets it through into the template detection stage.

The template pairs filter does not seem to have much effect on the accuracy of the speed estimation algorithm. If anything it probably makes it a bit less accurate. This is also the case when it is used in conjunction with the pre-template filters.

A.3 Experiment to compare Template model response with Reichardt correlator response using Vision Egg

The experiments conducted in Chapter 4 to compare the template model response to the Dror's elaborated Reichardt model and the response of the HSNE neuron with the rotating drum has been repeated here using the vision egg software. For this experiment, we generated pictures with square black shapes on a white background using MATLAB.

These square black shapes are random horizontal texture elements ('texels') and different sizes can be produced by changing the texture density parameter in the MATLAB code.

The CMOS camera was then subjected to these pictures with different texture density at a fixed distance of 17 cm on Vision Egg. Using Vision Egg, we could increase or decrease the speeds at which the pictures revolve around the CMOS camera. Our program then counts the average number of templates which are produced by detecting the movement of the texels. The average template count is obtained by averaging the total number of templates over 1000 frames. The procedure is repeated for five different texture densities over a range of speeds. The response of the Horridge template model is measured in the form of templates, so the velocity response curve to be plotted will be the velocity obtained from Vision Egg versus the template counts obtained from the software. A velocity response curve is plotted for each texture density and they can be found in Figure A.14.

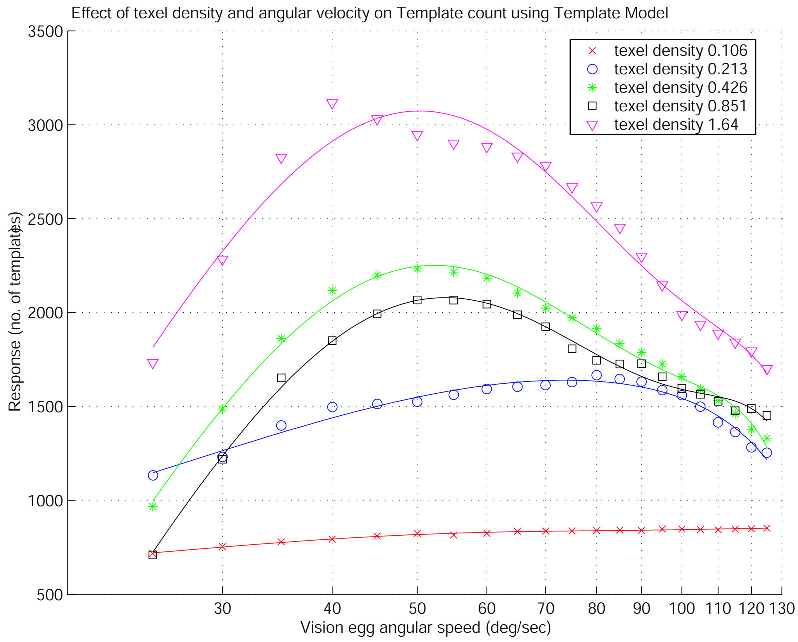

Fig. A.14. Velocity response curves measured at five different texture densities with the Horridge template model using Vision Egg stimuli. For all the curves, it can be seen that the response increases at lower velocities. This is due to the fact that as velocity is increased, more texels pass in front of the CMOS camera in a shorter time interval, resulting in the increase in response. However, the most of the curves level off and reach their optimum template count at around 50°/s. From this point, the response starts to decrease rapidly as velocity increases. This occurs because of the blurring effect caused by the fast motion of texels.

From Figure A.14, we can see that for all the curves, the response increases at lower velocities. This is due to the fact that as velocity is increased, more texels pass in front of the CMOS camera in a shorter time interval, resulting in the increase in response. However, the most of the curves level off and reach their optimum template count at around 50°/s. From this point, the response starts to decrease rapidly as velocity increases. This occurs because of the blurring effect caused by the fast motion of texels [Rajesh et al., 2004]. The higher the texture density, the lower the velocity at which the blur occurs. As the template model is used for motion detection, the motion of the texels is detected as edges. At low texture densities, the texels are bigger and fewer in number. There are also a smaller number of edges and thus fewer templates at low velocities. However, as the texture density increases, the number of edges detected and the number of templates counted increases. This results in the curve shifting to the left with increasing texture density. This shows that it has a similar response to the velocity response curves of both the Reichardt correlator and the HSNE neuron presented in Chapter 3. We can also see that the results are more consistent and with less variation than the velocity response curves in Figure 4.1, shown in Chapter 4.

A reason for the better results obtained could be attributed to the use of Vision Egg stimuli instead of stimuli stuck on the inside of a rotating cylinder. By using Vision Egg, the angular speeds of the stimuli were always consistent and very accurate. But for the rotating cylinder, the angular speeds were controlled by the voltage supply to the motor, thus the speeds were not as consistent and this has resulted in the variations found in Figure 4.1.

To go a further step in comparing the velocity response curves, we have normalized the curves in Figure A.14 to a maximum value of 1.0. This is shown in Figure A.15.

From Figure A.15, we can see the same characteristics like in Figure A.14, with the response rising to a peak response at an optimal velocity and then falling off. For Figure A.15, the shifting of curves to the left as texture density increases is also more obvious than that of Figure A.14. This compares very favourably with the velocity response curves of the model correlator and the wide-field neuron of the hoverfly presented in Chapter 3. With the normalization, we can also see that the curves cease to shift to the left at the very highest densities. This is also evident in the velocity response curves of the model correlator and the wide-field neuron of the hoverfly found in Figure 3.4 and Figure3.5 respectively shown in Chapter 3.

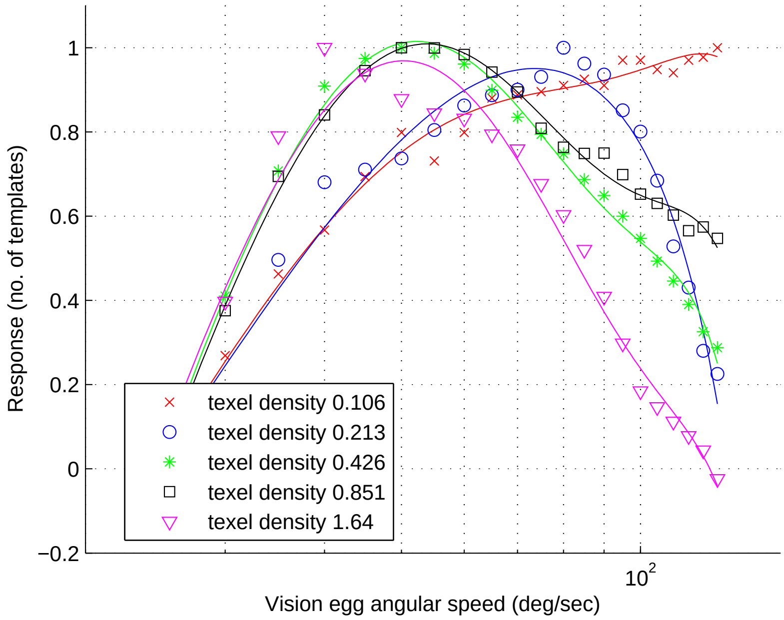

Fig. A.15. Normalized velocity response curves measured at five different texture densities using the Horridge template model. To go a further step in comparing the velocity response curves, we have normalized the curves in Figure A.14 to a maximum value of 1.0.

In order to understand the velocity performance of the template model using the the texel images, we used the Vision Egg to display the textures of different densities at different speeds instead of using a rotating cylinder stuck with the random texture elements as stimuli. Our vision software estimates the angular velocity of the moving texels using the template model algorithm and the results are shown in Figure A.16. The horizontal axis represents the actual angular velocity of the texels obtained from Vision Egg and the vertical axis represents the measured angular velocities estimated by our software.

From Figure A.16, we can see that at velocities below 125°/s, all the lines lie almost exactly on the ideal line. It has been expected that there will be a slight deviation of lines from the ideal line at lower velocities due to the presence of noise in the system. At higher velocities, the lines deviate away from the ideal line and this is particularly true as texture density increases. This occurs because at higher velocities, the edges are not clearly identified due to the blurring effect caused by the fast motion of texels.

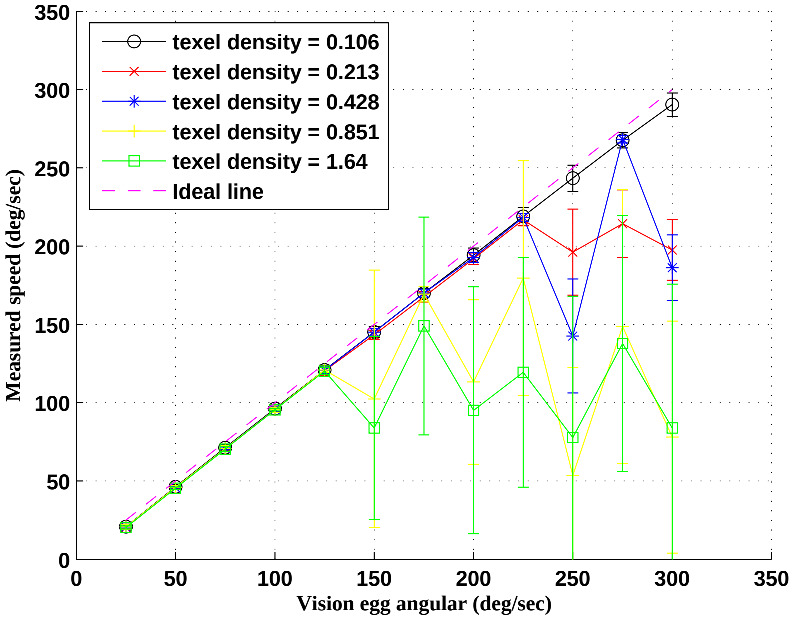

Fig. A.16. Benchmark angular velocity presented by the vision egg experiment versus angular velocity determined by insect vision system. It can be seen that at velocities below 125°/s, all the lines lie almost exactly on the ideal line. It has been expected that there will be a slight deviation of lines from the ideal line at lower velocities due to the presence of noise in the system. At higher velocities, the lines deviate away from the ideal line and this is particularly true as texture density increases and this is due to the blurring effect caused by the fast motion of texels.

A.4 Conclusion

Velocity estimation forms an important part of our insect Vision research and the comparisons made above focuses mainly on the reliability of the template model to accurately estimate velocity. The velocity response curves of the template model should be similar to those of the model correlator as both models are developed from an EMD. This has been proven to be true as both models have very similar responses. Experiments done on the wide-field neuron of the hoverfly have also verified the results obtained for the model correlator and our implementation of the template model as several important characteristics present in the curves of the wide-field neuron have been matched. The results obtained from Vision egg experiments are found to be more obvious and more conclusive than the velocity response curves using the drum. This is mainly due to the use of Vision Egg as stimulus compared to the rotating cylinder that did not always rotate at consistent speeds.

For the estimation of velocities using the template model, vision egg implementation fares better in many aspects when compared to the drum method. At lower velocities, vision egg experiment gives a more accurate estimation of velocity. However at higher velocities, only those with lower texture densities continue to provide accurate estimations. As the texture density increases, the estimations become less accurate at high velocities.

Bibliography

ABBOTT-D (2001). Focus issue on unsolved problems of noise and fluctuations, *Chaos*, **11**(3), pp. 526–538.

ABBOTT-D, MOINI-A, BOUZERDOUM-A, NGUYEN-X. T, BLANKSBY-A, KIM-G, BOGNER-R. E AND ESHRAGHIAN-K (1994). A new VLSI smart sensor for collision avoidance inspired by insect vision, *Proceedings of SPIE, Intelligent Vehicle Highway Systems*, Boston, **2344**, pp. 105–115.

ADELSON-E. H AND BERGEN-J (1985). Spatiotemporal energy models for the perception of motion, *Journal of the Optical Society of America A*, **2**, pp. 284–299.

ALLIK-J AND PULVER-A (1995). Contrast response of a movement-encoding system, *Journal of Optical Society of America A*, **12**, pp. 1185–1197.

BADIA-S. B, PYK-P AND VERSCHURE-P. F. M. J (2007). A fly locust based neuronal control system applied to an unmanned aerial vehicle: the invertebrate neuronal principles for course stabilisation, altitude control and collision avoidance, *The International Journal of Robotics Research*, **26**(7), pp. 759–772.

BARLOW-H. B AND HILL-R. M (1963). Evidence for a physiological explanation of the waterfall phenomenon and figural after-effects, *Nature*, **200**, pp. 1345–1347.

BARLOW-H. B AND LEWICK-W. R (1965). The mechanism of directionally selective units in the rabbit's retina, *Journal of Physiology*, London, **178**, pp. 477–504.

BEARE-R, BLANKSBY-A AND BOUZERDOUM-A (1995). Low level visual motion processing using local motion detectors, *Proceedings IEEE International Conference on Neural Networks*, Perth, Australia, **1**, pp. 1–6.

BECKERS-U, EGELHAAF-M AND KURTZ-R (2007). Synapses in the fly motion-vision pathway: Evidence for a broad range of signal amplitudes and dynamics, *Journal of Neurophysiology*, **97**, pp. 2032–2041.

BOEDDEKER-N, LINDEMANN-J. P, EGELHAAF-M AND ZEIL-J (2005). Responses of blowfly motion-sensitive neurons to reconstructed optic flow along outdoor flight paths, *Journal of Comparative Physiology A*, **191**, pp. 1143–1155.

BORST-A (2007). Correlation versus gradient type motion detectors: the pros and cons, *Philosophical Transactions of the Royal Society of London, Series B, Biological Sciences*, **362**(1479), pp. 368–374.

BORST-A AND EGELHAAF-M (1987). Temporal modulation of luminance adapts time constant of fly movement detectors, *Biological Cybernetics*, **56**, pp. 209–215.

BORST-A AND EGELHAAF-M (1989). Principles of visual motion detection, *Trends in Neurosciences*, **12**(8), pp. 297–306.

BORST-A AND EGELHAAF-M (1992). *In vivo* imaging of calcium acculation in fly interneuronsas elicited by visual motion stimulation, *Proceedings of the National Academy of Sciences of the United States of America*, **89**(9), pp. 4139–4143.

BORST-A AND EGELHAAF-M (1994). Dendritic processing of synaptic information by sensory interneurons, *Trends In Neurosciences*, **17**, pp. 257–263.

BORST-A AND HAAG-J (2007). Optic flow processing in the cockpit of the fly, *Invertebrate Neurobiology (Cold Spring Harbour Labour)*, **1**, pp. 102–122.

BOUZERDOUM-A AND PINTER-R. B (1993). Shunting inhibitory cellular neural networks: derivation and stability analysis, *IEEE Transactions on Circuits and Systems I: Fundamental Theory and Applications*, **40**(3), pp. 215–221.

BRACEWELL-R (1999). *The Hilbert Transform*, 3rd ed. New York edn, McGraw-Hill.

BRINKWORTH-R. S. A AND O'CARROLL-D. C (2007). Biomimetic motion detection, *Proceedings of the ISSNIP*, **3**, pp. 137–142.

BUCHNER-E (1976). Elementary movement detectors in an insect visual system, *Biological Cybernetics*, **24**, pp. 85–101.

BUCHNER-E (1984). Behavioural analysis of spatial vision in insects, *Photoreception and Vision in Invertebrates*, pp. 561–621.

BUDIMIR-A, CORRELL-S, RAJESH-S AND ABBOTT-D (2004). Implementation of insect vision based motion detection models using a video camera, *Proceedings of the SPIE Conference on Smart Structures, Devices and Systems II*, **5649**, pp. 596–606.

BURROWS-M (1996). *The Neurobiology of an Insect Brain*, Oxford University Press.

BURTON-G. J AND MOORHEAD-I. R (1987). Color and spatial structure in natural scenes, *Applied Optics*, **26**, pp. 157–170.

CHIN-K AND ABBOTT-D (1999). Motion detection using color templates, *Proceedings of SPIE*, **3893**, pp. 314–321.

CLATWORTHY-P. L, CHIRIMUUTA-M, LAURITZEN-J. S AND TOLHURST-D. J (2003). Coding of the contrasts in natural images by populations of neurons in primary visual cortex (v1), *Vision Research*, **43**, pp. 1983–2001.

CLIFFORD-C. W. G AND LANGLEY-K (1995). A model of temporal adaptation in fly motion vision, *Vision Research*, **36**(16), pp. 2595–2608.

CLIFFORD-C. W. G AND LANGLEY-K (1997). An adaptive reichardt detector model of motion adaptation in insects and mammals, *Visual Neuroscience*, **14**(4), pp. 741–749.

COURELLIS-S. H AND MARMARELIS-V. Z (1990). An artificial neural network for motion detection and speed estimation, *Proceedings of the International Joint Conference on Neural Networks*, pp. 407–421.

CUNTZ-H, HAAG-J, FORSTNER-F, SEGEV-I AND BORST-A (2007). Robust coding of flow-field parameters by axo-axonal gap junctions between fly visual interneurons, *Proceedings of the National Academy of Sciences (PNAS)*, **104**(24), pp. 10229–10233.

DAUGMAN-J. D (1988). Complete discrete 2-d gabor transforms by neural networks for image analysis and compression, *IEEE Transactions on Acoustics, Speech, and Signal Processing*, **36**, pp. 1169–1179.

DELCOMYN-F (1998). *Foundation of Neurobiology*, W. H. Freeman and Company.

DE RUYTER VAN STEVENINCK-R. R, ZAAGMAN-W AND MASTEBROEK-H. A. K (1986). Adaptation of transient responses of a movement sensitive neuron in the visual system of blowfly *Caliphora erythrocephala*, *Biological Cybernetics*, **54**, pp. 223–236.

DONG-D. W AND ATTICK-J. J (1995). Statistics of natural time-varying images, *Network: Computation in Neural Systems*, **6**(3), pp. 345–358.

DOUGLASS-J. K AND STRAUSFELD-N. J (1995). Visual motion detection circuits in flies: peripheral motion computation by identified small-field retinotopic neurons, *Journal of Neuroscience*, **15**(8), pp. 5596–5611.

DROR-R. O (1998). *Accuracy of visual velocity estimation by* R*eichardt correlators*, Master's thesis, University of Cambridge, Cambridge, UK.

DROR-R. O, O'CARROLL-D. C AND LAUGHLIN-S. B (2000). The role of natural image statistics in biological motion estimation, *Proceedings of the IEEE International Workshop on Biologically Motivated Computer Vision*, Seoul, Korea, **1811**, pp. 492–501.

DROR-R. O, O'CARROLL-D. C AND LAUGHLIN-S. B (2001). Accuracy of velocity estimation by Reichardt correlators, *Journal of the Optical Society of America A*, **18**(2), pp. 241–252.

ECKERT-H (1981). The horizontal cells in the lobula plate of the blowfly, *Phaenicia sericata*, *Journal of Comparitive Physiology A*, **143**, pp. 511–526.

EGELHAAF-M (1985). On the neuronal basis of figure-ground discrimination by relative motion in the visual system of the fly ii. figure-detection cells , a new class of visual interneurons, *Biological Cybernetics*, **52**, pp. 195–209.

EGELHAAF-M AND BORST-A (1989). Transient and steady state response properties of movement detectors, *Journal of the Optical Society of America A*, **6**, pp. 116–127.

EGELHAAF-M AND REICHARDT-W (1987). Dynamic response properties of movement detectors - theoritical analysis and electrophysiological investigation in the visual system of fly, *Biological Cybernetics*, **56**(2-3), pp. 69–87.

EGELHAAF-M, BODDEKER-N, KERN-R, KRETZBERG-J, LINDEMANN-J. P AND WARZECHA-A. K (2003). Visually guided orientation in flies: case studies in computational neuroethology, *Journal of Comparative Physiology A*, **189**(6), pp. 410–409.

EGELHAAF-M, BORST-A AND REICHARDT-W (1989). Computational structure of a biological motion detection system as revealed by local detector analysis in the fly's nervous system, *Journal of the Optical Society of America A*, **6**, pp. 1070–1087.

EGELHAAF-M, KERN-R, KRAPP-H. G, KRETZBERG-J, KURTZ-R AND WARZECHA-A. K (2002). Neural encoding of behaviourally relevant visual motion information in the fly, *Trends in Neurosciences*, **25**(2), pp. 96–102.

EGGERMONT-J. J (2001). Between sound and perception: reviewing the search for a neural code, *Hearing Research*, **157**(1-2), pp. 1–42.

EMERSON-R. C, CITRON-M. C, VAUGHN-W. J AND KLEIN-S. A (1987). Nonlinear directionally selective subunits in complex cells of cat striate cortex, *Journal of Neurophysiology*, **58**, pp. 33–65.

EXNER-S (1894). Entwurf zu einer physiologischen erklrung der psychischen erscheinungen, *Teil. Deuticke, Leipzig*, p. 37140.

FARROW-K, HAAG-J AND BORST-A (2006). Non-linear, binocular interactions underlying flow field selectivity of a motion-sensitive neuron, *Nature Neuroscience*, **9**, pp. 1312–1320.

FERMI-G AND REICHARDT-W. E (1963). Optomotorische reaktionen der fliege musca domestica, *Kybernetik*, **2**, pp. 15–28.

FIELD-D. J (1987). Relations between the statistics of natural images and the response properties of cortical cells, *Journal of Optical Society of America A*, **4**, pp. 2379–2394.

FLEET-D. J AND JEPSON-A. D (1985). Spatiotemporal inseparability in early vision: centre-surround models and velocity selectivity, *Computational Intelligence*, **1**(3), pp. 89–102.

FLEET-D. J, WAGNER-H AND HEEGER-D. J (1996). Neural encoding of binocular disparity: energy model, position shifts and phase shifts, *Vision Research*, **36**(12), pp. 1839–1857.

FRANCESCHINI-N, RUFFIER-F AND SERRES-J (2007). A bio-inspired flying robots sheds light on insect piloting abilities, *Current Biology*, **17**(4), pp. 329–335.

FRANZ-M. O AND CHAHL-J. S (2002). Insect-inspired estimation of self-motion, *Lecture Notes in Computer Science (Biologically Motivated Computer Vision, Proceedings)*, **2525**, pp. 171–180.

FRANZ-M. O AND KRAPP-H. G (2000). Wide-field, motion sensitive neurons and matched filters for optic flow, *Biological Cybernetics*, **83**, pp. 185–197.

FYRE-M. A AND DICKINSON-M. H (2001). Fly flight: A model for the neural control of complex behaviour, *Neuron*, **32**, pp. 385–388.

GILBERT-C AND STRAUSFELD-N. J (1991). The functional organization of male-specific visual neurons in flies, *Journal of Comparative Physiology A*, **169**, pp. 395–411.

GREWE-J, MATOS-N, EGELHAAF-M AND WARZECHA-A (2006). Implications of functionally different synaptic inputs for neuronal gain and computational properties of fly visual interneurons, *Journal of Neurophysiology*, **96**, pp. 1838–1847.

GUZINSKI-R, NGUYEN-K, YONG-Z. H, RAJESH-S, CARROLL-D. C. O AND ABBOTT-D (2006). Characterization of insect vision based collision avoidance models using a video camera, *Proceedings of the SPIE Conference on Biomedical Applications of Micro and Nanoengineering II*, **6036**, p. 60361D.

HAAG-J, DENK-W AND BORST-A (2004). Fly motion vision is based on reichardt detectors regardless of the signal-to-noise ratio, *Proceedings of the National Academy of Sciences of the United States of America*, **101**(46), p. 1633316338.

HAAG-J, WERTZ-A AND BORST-A (2007). Integration of lobula plate output signals by dnovs1, an identified premotor descending neuron, *The Journal of Neuroscience*, **27**(8), pp. 1992–2000.

HARDIE-R. C (1985). Functional organisation of the fly retina, *Progress in Sensory Physiology*, **5**, pp. 1–80.

HARMER-G. P AND ABBOTT-D (Dec 2001). Motion detection and stochastic resonance in noisy environments, *Microelectronics Journal*, **32**(12), pp. 959–967.

HARRIS-R. A, O'CARROLL-D. C AND LAUGHLIN-S. B (1999). Adaptation and the temporal delay filter of fly motion detectors, *Vision Research*, **39**, pp. 2603–2613.

HARRIS-R. A, O'CARROLL-D. C AND LAUGHLIN-S. B (2000). Contrast gain reduction in fly motion adaptation, *Neuron*, **28**, pp. 595–606.

HASSENSTEIN-B AND REICHARDT-W (1956). Structure of a mechanism of perception of optical movement, *Proceedings of the 1st International Conference on Cybernetics*, pp. 797–801.

HAUSEN-K (1982a). The lobula complex of the fly: Structure, function and significance in visual behaviour, *In M. A. Ali(Eds.) Photoreception and vision in invertebrates*, **46**, pp. 67–79 (Plenum Press, New york).

HAUSEN-K (1982b). Motion sensitive interneurons in the optomotor system of the fly: The horizontal cells: Structure and signals, *Biological Cybernetics*, **45**(2), pp. 143–156.

HAUSEN-K (1982c). Motion sensitive interneurons in the optomotor system of the fly: The horizontal cells: Receptive field organisation and response characteristics, *Biological Cybernetics*, **46**(1), pp. 67–79.

HAUSEN-K AND EGELHAAF-M (1989). Neural mechanisms of visual course control in insects, *Facets in Vision*, edited by R. Hardie and D. Stavenga, Springer-Verlag, Berlin.

HAUSEN-K AND HENGSTENBERG-R (1987). Multimodal convergence of sensory pathways on motor neurons of flight muscles in the fly *Calliphora*, *Society for Neuroscience Abstracts*, **13**, p. 1059.

HEEGER-D. J (1987). Model for extraction of image flow, *Journal of Optical society of America A*, **4**, pp. 1455–1471.

HEISENBERG-M AND WOLF-R (1988). Reafferent control of optomotor yaw torque in *Drosophila melanogastor*, *Journal of Comparative Physiology*, **163**(3), pp. 338–340.

HENGSTENBERG-R (1982). Common visual response properties of giant vertical cells in the lobula plate of the blow fly *Calliphora*, *Journal of Comparative Physiology A*, **149**, pp. 179–193.

HENGSTENBERG-R (1998). Controlling the fly's gyroscopes, *Nature*, **392**, pp. 757–758.

HENGSTENBERG-R, HAUSEN-K AND HENGSTENBERG-B (1982). The number and structure of giant vertical cells (vs) in the lobula plate of the blowfly *Calliphora eythrocephala*, *Journal of Comparative Physiology A*, **149**, pp. 163–177.

HORN-B. K. P AND SCHUNCK-B. G (1981). Determining optical flow, *Artificial Intelligence*, **17**, pp. 185–203.

HORRIDGE-G. A (1990). A template theory to relate visual processing, *Proceedings of the Royal Society of London B*, **239**, pp. 17–33.

HOWARD-J. H, DUBS-A AND PAYNE-R (1984). The dynamics of phototransduction in insects, *Journal of Comparative Physiology*, **154**, pp. 707–718.

IBBOTSON-M. R, CLIFFORD-C. W. G AND MARK-R. F (1998). Adaptation to visual motion in directional neurons of the nucleus of the optic tract, *Journal of Neurophysiology*, **79**, pp. 1481–1493.

IBBOTSON-M. R, MARK-R. F AND MADDESS-T. L (1994). Spatiotemporal response properties of direction-selective neurons in the nuecleus of optic tract and dorsal terminal nucleus of the wallaby *Macropus - Eugenii*, *Journal of Neurophysiology*, **72**, pp. 2927–2943.

JAMES-A. C (1990). *White-Noise Studies in the Fly Lamina*, PhD thesis, Australian National University.

JARVILEHTO-M (1985). The eye: Vision and perception, *Comprehensive Insect Physiology Biochemistry and Pharmacology - Nervous system: Sensory*, **6**, pp. 355–429.

KARMEIER-K, VAN HATEREN-J. H, KERN-R AND EGELHAAF-M (2006). Encoding of naturalistic optic flow by a population of blowfly motion-sensitive neurons, *Journal of Neurophysiology*, **96**, pp. 1602–1614.

KERN-R, VAN HETEREN-J. H, MICHAELIS-C, LINDEMANN-J. P AND EGELHAAF-M (2005). Function of a fly motion-sensitive neuron matches eye movements during free flight, *Public Library of Science - Biology*, **3**(6), pp. 1130–1138.

KIMMERLE-B AND EGELEHAAF-M (2000). Detection of object motion by a fly neuron during simulated flight, *Journal of Comparative Physiology A*, **186**, pp. 21–31.

KIRSCHFELD-K (1972). The visual system of Musca: studies on optics, structure and function, *Information Processing in the Visual Systems of Arthropods*, edited by R. Wehner, Springer-Verlag, Berlin.

KOENDERINK-J. J AND VAN DOORN-A. J (1987). Facts on optic flow, *Biological Cybernetics*, **56**(4), pp. 247–254.

KRAPP-H. G AND HENGSTENBERG-R (1996). Estimation of self-motion by optic flow processing in single visual interneurons, *Nature*, **384**(6608), pp. 463–466.

KRAPP-H. G, HENGSTENBERG-B AND HENGSTENBERG-R (1998). Dendritic structure and receptive field organisation of optic flow processing interneurons in the fly, *Journal of Neurophysiology*, **79**, pp. 1902–1917.

KRAPP-H. G, HENGSTENBERG-R AND EGELHAAF-M (2001). Binocular contributions to optic flow processing in the fly visual system, *Journal of Neurophysiology*, **85**(2), pp. 724–734.

LAND-M. F AND ECKERT-H. M (1985). Maps of the acute zones of fly eyes, *Journal of Comparitive Physiology*, **156**, pp. 525–538.

LANGER-M. S (2000). Large-scale failures of f(-alpha) scaling in natural image spectra, *Journal of Optical Society of America A*, **17**(1), pp. 28–33.

LAUGHLIN-S. B (1981). A simple coding procedure enhances a neuron's information capacity, *Z. Naturforsch. (C)*, **36**, pp. 910–912.

LAUGHLIN-S. B (1994). Matching coding, circuits, cells and molecules to signals: general principles of retinal design in the fly's eye, *Progress in Retinal Research*, **13**, pp. 165–195.

LAUGHLIN-S. B (1996). Matched filtering by a photoreceptor membrane, *Vision Research*, **36**(11), pp. 1529–1541.

LEHRER-M, SRINIVASAN-M. V, ZHANG-S. W AND HORRIDGE-G. A (1998). Motion cues provide the bees visual world with three dimension, *Nature*, **332**, pp. 356–357.

LEWEN-G. D, BIALEK-W AND DE RUYTER VAN STEVENINCK-R. R (2001). Neural coding of naturalistic motion stimuli, *Network: Computation in Neural Systems*, **12**(3), pp. 317–329.

LINDEMANN-J. P, KERN-R, MICHAELIS-C, MEYER-P, VAN HETERN-J. H AND EGELHAAF-M (2003). Flimax, a novel stimulus device for panoramic and high speed presentation of behaviourally generated optic flow, *Vision Research*, **43**(7), pp. 779–791.

MADDESS-T AND LAUGHLIN-S. B (1985). Adaptation of the motion sensitive neuron H1 is generated locally and governed by contrast frequency, *Proceedings of the Royal Society of London B*, **225**, pp. 251–275.

MARR-D AND HILDRETH-E (1980). Theory of edge detection, *Proceedings of the Royal Society of London B*, **207**, pp. 187–217.

MASTEBROEK-H. A. K, ZAAGMAN-W. H AND LENTING-B. P. M (1980). Motion detection: performance of a wide field element in visual system of the blowfly, *Vision Research*, **20**, pp. 467–474.

MCCANN-G. D AND ARNETT-D. W (1972). Spectral and polarization sensitivity of the dipteran visual system, *The Journal of General Physiology*, **59**, pp. 534–558.

MCKEE-S. P, SILVERMAN-G. H AND NAKAYAMA-K (1986). Precise velocity discrimination despite random variation in temporal frequency and contrast, *Vision Research*, **26**, pp. 609–619.

MOINI-A AND BOUZERDOUM-A (1997). A biologically motivated imager and motion detector with pixel level image processing, *Australian Microelectronics Conference*, Melbourne, Australia, pp. 180–185.

MOINI-A, BLANKSBY-A, BOUZERDOUM-A, ESHRAGHIAN-K AND BEARE-R (1995). Multiplicative noise cancellation (mnc) for analog VLSI sensors, *ETD 2000, Electronic Technology Directions of the Year 2000*, **1**, pp. 253–257.

MOINI-A, BOUZERDOUM-A, ESHRAGHIAN-K, YAKOVLEFF-A, NGUYEN-X. T, BLANKSBY-A, BEARE-R, ABBOTT-D AND BOGNER-R. E (1997). An insect vision based motion detection chip, *IEEE Journal of Solid State Circuits*, **32**(2), pp. 279–284.

MOINI-A, BOUZERDOUM-A, YAKOVLEFF-A, ABBOTT-D, KIM-O, ESHRAGHIAN-K AND BOGNER-R. E (1993). An analog implementation of early visual processing in insects, *Proceeding of the International Symposium of* VLSI *technology, Systems and Applications*, **1**, pp. 283–287.

MOINI-A, BOUZERDOUM-A, YAKOVLEFF-A AND ESHRAGHIAN-K (1996). A two dimensional motion detector based on insect vision, *Advanced Focal Plane Arrays and Electronic Cameras*, Berlin, Germany, pp. 146–157.

NAKAYAMA-K (1985). Biological image motion processing — a review, *Vision Research*, **25**(5), pp. 625–660.

NALBACH-G AND HENGSTENBERG-R (1994). The halteres of the blowfly *Calliphora*: Three dimentional organisation of compensatory reaction to real and simulated rotations, *Journal of Comparitive Physiology A*, **175**, pp. 695–708.

NEMENMAN-I, LEWEN-G. D, BIALEK-W AND DE RUYTER VAN STEVENINCK-R. R (2007). Neural coding of natural stimuli: Uncovering information at sub-millisecond resolution, *BMC Neuroscience*.

NGUYEN-H, RAJESH-S AND ABBOTT-D (2001). Motion detection algorithms using template model, *Proceedings of the SPIE Conference on Electronics and Structures for MEMS II*, Adelaide, Australia, **5279**, pp. 78–90.

NGUYEN-X. T (1995). *Smart VLSI Micro-Sensors for Velocity Estimation Inspired by Insect Vision*, PhD thesis, EEE Department,University of Adelaide.

NGUYEN-X. T, BOUZERDOUM-A AND MOINI-A (1996). Velocity measurement using a smart microsensor, *International Symposium on Robotics and Cybernetics*, Lille, France, **943**, pp. 937–942.

NGUYEN-X. T, BOUZERDOUM-A, BOGNER-R. E, MOINI-A, ESHRAGHIAN-K AND ABBOTT-D (1993). The stair-step tracking algorithm for velocity estimation, *Proceedings of the Australian New Zealand Conference on Intelligent Information Systems*, Perth, Australia, pp. 412–416.

NIVEN-J. E, ANDERSON-J. C AND LAUGHLIN-S. B (2007). Fly photoreceptors demonstrate energy information trade offs in neural coding, *PLOS Biology*, **5**(4), pp. 828–840.

NORDSTORM-K, BARNETT-P. D, DE MIGUEL-I. M, BRINKWORTH-R. S. A AND O'CARROLL-D. C (2007). Sexual dimorphism in the hoverfly visual system with a male hsn neuron tuned to rotational optic flow, *In preparation*.

O'CARROLL-D. C, BIDWELL-N. J, LAUGHLIN-S. B AND WARRANT-E. J (1996). Insect motion detectors matched to visual ecology, *Nature*, **382**, pp. 63–66.

O'CARROLL-D. C, LAUGHLIN-S. B, BIDWELL-N. J AND HARRIS-R. A (1997). Spatio-temporal properties of motion detectors matched to low image velocities in hovering insects, *Vision Research*, **37**, pp. 3427–3439.

PAYNE-R AND HOWARD-J (1981). Response of an insect photoreceptor: a simple log-normal model, *Nature*, **290**, pp. 415–416.

PETROV-Y AND ZHAOPING-L (2003). Local correlations, information redundancy and sufficient pixel depth in natural images, *Journal of Optical Society of America A*, **20**(1), pp. 56–66.

PIERANTONI-R (1976). A look into the cock-pit of the fly: the architecture of the lobula plate, *Cell and Tissue Research*, **171**, pp. 101–122.

PINTER-R. B (1984). Adaptation of receptive field spatial organization via multiplicative lateral inhibition, *Proceedings of the the IEEE Conference on Systems, Man and Cybernetics*, pp. 328–331.

RAJESH-S, ABBOTT-D AND O'CARROLL-D. C (2006). A 16 pixel yaw sensor for velocity estimation, *Proceedings of the SPIE conference on BioMEMS and Nanotechnology II*, **6036**, p. 603618.

RAJESH-S, CARROLL-D. C. O AND ABBOTT-D (2002). Elaborated reichardt correlators for velocity estimation tasks, *Proceedings of the SPIE Conference on Biomedical Applications of Micro and Nanoengineering*, Melbourne, Australia, **4937**, pp. 241–253.

RAJESH-S, CARROLL-D. C. O AND ABBOTT-D (2003). Velocity estimation and comparison of two insect vision based motion detection model, *Proceedings of the SPIE Conference on Smart Materials, Structures and Systems,* Bangalore, India, **5062**, pp. 401–412.

RAJESH-S, CARROLL-D. C. O AND ABBOTT-D (2004). Effects of nonlinear elaborations on the performance of a reichardt correlator, *Proceedings of the SPIE Conference on BioMEMS and Nanotechnology*, **5279**, pp. 287–303.

RAJESH-S, CARROLL-D. C. O AND ABBOTT-D (2005a). Man made velocity estimators based on insect vision, *Smart Materials and Structures*, **14**, pp. 413–424.

RAJESH-S, RAINSFORD-T AND O'CARROLL-D. C (2005b). Modelling pattern noise in responses of fly motion detectors to naturalistic scenes, *Proceedings of the SPIE Conference on Biomedical Applications of Micro- and Nano-engineering II*, **5651**, pp. 160–173.

RAJESH-S, RAINSFORD-T, BRINKWORTH-R. S. A, ABBOTT-D AND O'CARROLL-D. C (2007). Implementation of saturation for modelling pattern noise using naturalistic stimuli, *Proceedings of the SPIE conference on BioMEMS and Nanotechnology II*, **6414**, p. 641424.

RAJESH-S, STRAW-A, O'CARROLL-D. C AND ABBOTT-D (2005c). Effect of spatial sampling on pattern noise in insect-based motion detection, *Proceedings of the SPIE conference on Smart Structures, Devices, and Systems II*, **5649**, pp. 811–825.

RAJESH-S, STRAW-A, O'CARROLL-D. C AND ABBOTT-D (2005d). Effects of compressive nonlinearity on insect-based motion detection, *Proceedings of the SPIE conference on Smart Structures, Devices, and Systems II*, **5649**, pp. 798–810.

RATLIFF-F AND HARTLINE-H. K (1974). *Studies on Excitation and Inhibition in Retina*, Chapman and Hall, London.

REICHARDT-W (1961). Autocorrelation, aprinciple for the evaluation of sensory information by the central nervous system, *Principles of Sensory Communication*, edited by A. Rosenblith, MIT Press and John Wiley and Sons, New York.

REIHLE-A AND FRANCESCHINI-N (1982). Response of a direction-selective, movement detecting neuron under precise stimulation of two identified photoreceptor cells, *Neuroscience Letters Supplement*, **10**, p. 411.

RUDERMAN-D. L (1994). The statistics of natural images, *Network: Computation in Neural System*, **5**, pp. 517–548.

RUDERMAN-D. L (1997). Origins of scaling in natural images, *Vision Research*, **37**(23), pp. 3385–3398.

RUDERMAN-D. L AND BIALEK-W (1994). Statistics of natural images: Scaling in the woods, *Physical Review Letters*, **73**(6), pp. 814–817.

SHOEMAKER-P. A, O'CARROLL-D. C AND STRAW-A (2001). Implementation of visual motion detection with contrast adaptation, *Proceedings of the SPIE conference on Microelectronics and Micro-Electro-Mechanical Systems,* Adelaide, Australia, **4591**, pp. 316–327.

SHOEMAKER-P. A, O'CARROLL-D. C AND STRAW-A (2005). Velocity constancy and models for wide-field visual motion detection in insects, *Biological Cybernetics*, **93**(4), pp. 275–287.

SIMONCELLI-E. P (2003). Vision and the statistics of the visual environment, *Current Opinion in Neurobiology*, **13**(2), pp. 144–149.

SIMONCELLI-E. P AND OLSHAUSEN-B. O (2001). Natural image statistics and neural representation, *Annual Review of Neuroscience*, **24**(1), pp. 193–216.

SINGLE-S AND BORST-A (1998). Dendritic integration and its role in computing image velocity, *Science*, **281**, pp. 1848–1850.

SNYDER-A. W, STAVENGA-D. G AND LAUGHLIN-S. B (1977). Spatial information capacity of compound eyes, *Journal of Comparative Physiology*, **116**, pp. 183–207.

SOBEY-P (1990). Determining range information from self motion - the template model, *Proceedings of the SPIE on Intelligent Robots and Computer Vision*, **1382**, pp. 123–131.

SRINIVASAN-M. V (1990). Generalised gradient schemes for the measurement of two dimensional image motion, *Biological Cybernetics*, **63**, pp. 421–431.

SRINIVASAN-M. V, LAUGHLIN-S. B AND DUBS-A (1982). Predictive coding - a fresh view of inhibition in the retina, *Proceedings of the Royal Society of London Series B - Biological Sciences*, **216**(1205), pp. 427–459.

SRINIVASAN-M. V, POTESER-M AND KRAL-K (1999). Motion detection in insect orientation and navigation, *Vision Research*, **39**(16), pp. 2749–2766.

SRINIVASAN-M. V, ZHANG-S. W, LEHRER-M AND COLLET-T. S (1996). Honeybee navigation en route to the goal: visual flight control and odometry, *Journal of Experimental Biology*, **199**, pp. 237–244.

STRAUSFELD-N. J AND BASSEMIR-U. K (1985). Lobula plate and ocellar interneurons converge onto a cluster of descending neurons leading to leg and neck motor neuropil in *Calliphora erythrocephala*, *Cell and Tissue Research*, **240**, pp. 617–640.

STRAUSFELD-N. J AND SEYAN-H. S (1985). Convergence of visual, haltere and prosternal inputs at neck motor neurons of *Calliphora erythrocephala*, *Cell and Tissue Research*, **240**, pp. 601–615.

STRAUSFELD-N. J, SEYAN-H. S AND MILDE-J. J (1987). The neck motor system of the fly *Calliphora erythrocephala* 1. muscles and motor neurons, *Journal of Comparitive Physiology A*, **160**, pp. 205–224.

STRAW-A (2004). *Neural responses to moving natural scenes*, PhD thesis, University of Adelaide, Australia.

TOLHURST-D. J, TADMOR-Y AND CHAO-T (1992). Amplitude spectra of natural images, *Ophthalmology and Physiological Optics*, **12**, pp. 229–232.

TOURYAN-J AND DAN-Y (2001). Analysis of sensory coding with complex stimuli, *Current Opinion in Neurobiology*, **11**(4), pp. 443–448.

TRISCHLER-C, BOEDDEKER-N AND EGELHAAF-M (2007). Characterisation of a blowfly male specific neuron using behaviourally generated visual stimuli, *Journal of Comparative Physiology A*, **193**(5), pp. 559–572.

van der Schaaf-A and van Hateren-J. H (1996). Modelling the power spectra of natural images: Statistics and information, *Vision Research*, **36**(17), pp. 2759–2770.

van Hateren-J. H (1990). Directional tuning curves, elementary movement detectors, and the estimation of the direction of visual motion, *Vision Research*, **30**, pp. 603–614.

van Hateren-J. H (1992). Theoritical predictions of spatiotemporal receptive fields of fly lmcs and experimental validation, *Journal of comparative Physiology A*, **171**, pp. 157–170.

van Hateren-J. H (1997). Processing of natural time series of intensities by the visual system of a blowfly, *Vision Research*, **37**, pp. 3407–3416.

van Hateren-J. H and Snippe-H. P (2001). Information theoritical evaluation of parametric models of gain control in blowfly photoreceptor cells, *Vision Research*, **41**(14), pp. 1851–1865.

van Santen-J. P and Sperling-G (1985a). Elaborated Reichardt detectors, *Journal of the Optical Society of America A*, **2**, pp. 300–321.

van Santen-J. P. H and Sperling-G (1985b). Elaborated reichardt dtetectors, *Journal of the Optical Society of America A*, **2**, pp. 300–321.

Watson-A. B and Ahumada-A. J (1985). Model of human visual-motion sensing, *Journal of the Optical Society of America A*, **2**(2), pp. 322–341.

Wehrhahn-C (1986). Motion sensitive yaw torque response of the housefly *Musca*: A quantitative study, *Biological Cybernetics*, **55**, pp. 275–280.

Wolf-Oberhollenzer-F and Kirschfeld-K (1994). Motion sensitivity in the nucleus of the basal optic root of the pigeon, *Journal of Neurophysiology*, **71**, pp. 1559–1573.

Yakovleff-A, Abbott-D, Nguyen-X. T and Eshraghian-K (1995). Obstacle avoidance and motion induced navigation, *Proceedings of the Computer Architecture for Machine Perception Workshop*, **1**, pp. 384–393.

Yakovleff-A and Moini-A (1997). Motion perception using analog VLSI, *Journal of Analog Integrated Circuits and Signal Processing*, **2**, pp. 1–22.

Yakovleff-A, Moini-A, Bouzerdoum-A, Nguyen-X. T, Bogner-R. E, Eshraghian-K and Abbott-D (1993). A micro sensor based on insect vision, *Proceedings of the Computer Architecture for Machine Perception workshop (CAMP'93)*, **15-17**, pp. 137–146.

Yakovleff-A, Nguyen-X. T, Bouzerdoum-A, Moini-A, Bogner-R. E and Eshraghian-K (1994). Dual-purpose interpretation of sensory information, *Proceedings IEEE International Conference on Robotics and Automation,* San Diego, USA,, **2**, pp. 1635–1640.

Glossary

Acronyms that follow are in the order that they appear in the Thesis.

2D – Two Dimensional

HS – Horizontal System

VS – Vertical System

HSN – Horizontal System North

HSE – Horizontal System Equatorial

HSS – Horizontal System South

FD – Feature Detecting

EMD – Elementary Motion Detectors

MLG – Male Specific Lobula Giant

CMOS – Complementary Metal Oxide Semiconductor

DMST – Directionally Motion Sensitive Template

PCT – Position Conjugate Template

VLSI – Very Large Scale Integration

AGC – Automatic Gain Control

RGB – Red Green Blue

MNC – Multiplicative Noise Cancellation

HSNE – Horizontal System North Equatorial

LMC – Lamina Monopolar cells

LPF – Low Pass Filter

TF – Temporal Filter

DF – Delay filter

CRT – Cathode Ray Tube

RAM – Random Access Memory

DDR – Double Data RAM

MB – Mega Byte

UAV – Unmanned Aerial Vehicle

3D – Three Dimensional

DC – Direct Current

LPTCs – Lobula Plate Tangential cells

LCD – Liquid Crystal Display

Resume

Sreeja Rajesh graduated from Bharathiyar University, India, with a First Class Bachelors in Engineering (Electrical and Electronic Engineering) in 1999. In 2000, Sreeja worked for Beonic corporation Pty. Ltd. (formerly called Traffic Pro Pty. Ltd.) with a team of research scientists to develop customer surveillance and people counting software using Insect vision based and Computer vision based algorithms. She commenced her PhD under the supervision of Prof Derek Abbott (School of Electrical and Electronic Engineering) and Prof David O' Carroll (School of Physiology) at the University of Adelaide. She was awarded a US Airforce and Sir Ross and Sir Keith Smith funded scholarship.

Sreeja Rajesh is a member of SPIE and OSA and has authored and coauthored more than 10 publications and has given more than 10 presentations at conferences including an invited talk at the ISSS Conference on Smart Materials and Structures, Bangalore, India. She is currently employed by the Defence Science and Technology Organization (DSTO) in Edinburgh, South Australia.

Scientific Genealogy

My scientific genealogy via one of my supervisors is as follows:

Sreeja Rajesh's Scientific Genealogy			
1774	MA	University of Cambridge	John Cranke
1782	MA	University of Cambridge	Thomas Jones
1811	MA	University of Cambridge	Adam Sedgwick
1830	MA	University of Cambridge	William Hopkins
1857	MA	University of Cambridge	Edward John Routh
1868	MA	University of Cambridge	John William Strutt (Lord Rayleigh)
1883	MA	University of Cambridge	Joseph John Thomson
1903	MA	University of Cambridge	John Sealy Townsend
1923	DPhil	University of Oxford	Victor Albert Bailey
1948	MSc	University of Sydney	Ronald Ernest Aitchison
1964	PhD	University of Sydney	Peter Harold Cole
1980	PhD	University of Adelaide	Kamran Eshraghian
1995	PhD	University of Adelaide	Derek Abbott
2007	PhD submitted	University of Adelaide	Sreeja Rajesh